

# A pan-African high-resolution drought index dataset

Jian Peng <sup>1,2</sup>, Simon Dadson <sup>1</sup>, Feyera Hirpa <sup>1</sup>, Ellen Dyer <sup>1</sup>, Thomas Lees <sup>1</sup>, Diego G. Miralles <sup>3</sup>, Sergio M. Vicente-Serrano <sup>4</sup>, Chris Funk <sup>5,6</sup>

1. School of Geography and the Environment, University of Oxford, OX1 3QY Oxford, UK;

2. Max Planck Institute for Meteorology, Hamburg, Germany;

3. Laboratory of Hydrology and Water Management, Ghent University, Ghent, Belgium;

4. Instituto Pirenaico de Ecología, Consejo Superior de Investigaciones Científicas (IPE-CSIC) Zaragoza, Spain;

5. U.S. Geological Survey, Earth Resources Observation and Science Center, Sioux Falls, South Dakota;

6. Santa Barbara Climate Hazards Center, University of California, USA;

Corresponding author: Jian Peng (jian.peng@ouce.ox.ac.uk)

## Abstract

Droughts in Africa cause severe problems such as crop failure, food shortages, famine, epidemics and even mass migration. To minimize the effects of drought on water and food security over Africa, a high-resolution drought dataset is essential to establish robust drought hazard probabilities and to assess drought vulnerability considering a multi- and cross-sectorial perspective that includes crops, hydrological systems, rangeland, and environmental systems. Such assessments are essential for policy makers, their advisors, and other stakeholders to respond to the pressing humanitarian issues caused by these environmental hazards. In this study, a high spatial resolution Standardized Precipitation-Evapotranspiration Index (SPEI) drought dataset is presented to support these assessments. We compute historical SPEI data based on Climate Hazards group InfraRed Precipitation with Station data (CHIRPS) precipitation estimates and Global Land Evaporation Amsterdam Model (GLEAM) potential evaporation estimates. The high resolution SPEI dataset (SPEI-HR) presented here spans from 1981 to 2016 (36 years) with 5 km spatial resolution over the whole Africa. To facilitate the diagnosis of droughts of different durations, accumulation periods from 1 to 48 months are provided. The quality of the resulting dataset was compared with coarse-resolution SPEI based on Climatic Research Unit (CRU) Time-Series (TS) datasets, and Normalized Difference Vegetation Index (NDVI) calculated from the Global Inventory Monitoring and Modeling System (GIMMS) project, as well as with root zone soil moisture modelled by GLEAM. Agreement found between coarse resolution SPEI

from CRU TS (SPEI-CRU) and the developed SPEI-HR provides confidence in the estimation of temporal and spatial variability of droughts in Africa with SPEI-HR. In addition, agreement of SPEI-HR versus NDVI and root zone soil moisture – with average correlation coefficient (R) of 0.54 and 0.77, respectively – further implies that SPEI-HR can provide valuable information to study drought-related processes and societal impacts at sub-basin and district scales in Africa. The dataset is archived in Centre for Environmental Data Analysis (CEDA) with link: <http://dx.doi.org/10.5285/bbdfd09a04304158b366777eba0d2aeb> (Peng et al., 2019a)

**Keywords:**

Drought, Africa, Precipitation, Potential evaporation, drought management, disaster risk reduction

62 Drought is a complex phenomenon that affects natural environments and socioeconomic systems in the  
63 world (von Hardenberg et al., 2001; Vicente-Serrano, 2007; Van Loon, 2015; Wilhite and Pulwarty, 2017).  
64 Impacts include crop failure, food shortage, famine, epidemics and even mass migration (Wilhite et al.,  
65 2007; Ding et al., 2011; Zhou et al., 2018). In recent years, severe events have occurred across the world,  
66 such as the 2003 central Europe drought (García-Herrera et al., 2010), the 2010 Russian drought (Spinoni et  
67 al., 2015), the 2011 Horn of Africa drought (Nicholson, 2014), the southeast Australian's Millennium  
68 drought (van Dijk et al., 2013; Peng et al., 2019d), the 2013/2014 California drought (Swain et al., 2014), the  
69 2014 North China drought (Wang and He, 2015) and the 2015–2017 Southern Africa drought (Baudoin et  
70 al., 2017; Muller, 2018). Widespread negative effects of these droughts on natural and socioeconomic  
71 systems have been reported afterwards (Wegren, 2011; Arpe et al., 2012; Griffin and Anchukaitis, 2014;  
72 Mann and Gleick, 2015; Dadson et al., 2019; Marvel et al., 2019). Thus, there is a clear need to improve our  
73 knowledge about the spatial and temporal variability of drought, which provides a basis for quantifying  
74 drought impacts and the exposure of society, the economy and the environment over different areas and  
75 time-scales (Pozzi et al., 2013; AghaKouchak et al., 2015).

76 Generally, drought is defined as a temporal anomaly characterized by a deficit of water compared with long-  
77 term conditions (Mishra and Singh, 2010; Van Loon, 2015). Droughts can typically be grouped into five  
78 types: meteorological (precipitation deficiency), agricultural (soil moisture deficiency), hydrological (runoff  
79 and/or groundwater deficiency), socioeconomic (social response to water supply and demand) and  
80 environmental or ecologic (Keyantash and Dracup, 2002; AghaKouchak et al., 2015; Crausbay et al., 2017).  
81 These different drought categories involve different event characteristics in terms of timing, intensity,  
82 duration, and spatial extent, making it very difficult to characterize droughts quantitatively (Panu and  
83 Sharma, 2002; Lloyd-Hughes, 2014; Vicente-Serrano, 2016). For this reason numerous drought indices have  
84 been proposed for precise applications, and reviews of the available indices have been provided by previous  
85 studies such as Heim Jr (2002), Keyantash and Dracup (2002), and Mukherjee et al. (2018). Van Loon

86 (2015) noted that there is no best drought index for all types of droughts, because every index is designed for  
87 a specific drought type, thus multiple indices are required to capture the multifaceted nature of drought.  
88 Nevertheless, the Standardized Precipitation Index (SPI) is recommended by the World Meteorological  
89 Organization (WMO) for drought monitoring, which is calculated based solely on long-term precipitation  
90 data over different time spans (McKee et al., 1993). The advantages of SPI are its relative simplicity and its  
91 ability to characterize different types of droughts given the different times of response of different usable  
92 water sources to precipitation deficits (Kumar et al., 2016; Zhao et al., 2017). However, information on  
93 precipitation is inadequate to characterize drought; in most definitions, drought conditions also depend on  
94 the demand of water vapor from the atmosphere. More recently, Vicente-Serrano et al. (2010) proposed an  
95 alternative drought index for SPI, which is called Standardized Precipitation Evapotranspiration Index  
96 (SPEI). Compared to SPI, it considers not only the precipitation supply, but also the atmospheric evaporative  
97 demand (Beguería et al., 2010; Vicente-Serrano et al., 2012b). This makes the index more informative of the  
98 actual drought effects over various natural systems and socioeconomic sectors (Vicente-Serrano et al., 2012b;  
99 Bachmair et al., 2016; Kumar et al., 2016; Sun et al., 2016c; Bachmair et al., 2018; Peña-Gallardo et al.,  
100 2018a; Peña-Gallardo et al., 2018b; Sun et al., 2018).

101 For the calculation of SPEI, high-quality and long-term observations of precipitation and atmospheric  
102 evaporative demand are necessary. These observations may either come from ground-based station data or  
103 gridded data such as satellite and reanalysis datasets. For example, the SPEIbase (Beguería et al., 2010) and  
104 the Global Precipitation Climatology Centre Drought Index (GPCC-DI) (Ziese et al., 2014) both provide  
105 SPEI datasets at global scale. The SPEIbase provides gridded SPEI with a 50-km spatial resolution, and is  
106 calculated from Climatic Research Unit (CRU) Time-Series (TS) datasets, which are produced based on  
107 measurements from more than 4000 ground-based weather stations over the world (Harris et al., 2014). The  
108 SPEI dataset provided by GPCC-DI has spatial resolution of 1°, and was generated from GPCC precipitation  
109 (Becker et al., 2013; Schneider et al., 2016) and National Oceanic and Atmospheric Administration  
110 (NOAA)'s Climate Prediction Center (CPC) temperature dataset (Fan and Van den Dool, 2008). Both of



111 these datasets have been applied for various drought related studies at global and regional scales (e.g., Chen  
112 et al., 2013; Vicente-Serrano et al., 2013; Isbell et al., 2015; Sun et al., 2016a; Vicente-Serrano et al., 2016;  
113 Deo et al., 2017). However, these global SPEI data sets' spatial resolution are too coarse to be applied at  
114 district or sub-basin scales (Vicente-Serrano et al., 2017). A sub-basin scale quantification of drought  
115 conditions is particularly crucial in regions such as Africa, in which geospatial data and drought indices can  
116 be essential to manage existing drought-related risks (Vicente-Serrano et al., 2012a) and where in-situ  
117 measurements are scarce (Trambauer et al., 2013; Masih et al., 2014; Anghileri et al., 2019). Over last  
118 century, Africa has been severely influenced by intense drought events, which has led to food shortages and  
119 famine in many countries (Anderson et al., 2012; Yuan et al., 2013; Sheffield et al., 2014; Awange et al.,  
120 2016; Funk et al., 2018; Nicholson, 2018; Gebremeskel et al., 2019). Therefore, the availability of a high-  
121 resolution drought index dataset may contribute to an improved characterization of drought risk and  
122 vulnerability, and minimize its impact on water and food security by supporting policy makers, water  
123 managers and stakeholders. Conveniently, with the advancement of satellite technology, the estimation of  
124 precipitation and evaporation from remote sensing datasets is becoming more accurate (Fisher et al., 2017).  
125 In particular, the long-term Climate Hazards group InfraRed Precipitation with Station data (CHIRPS) (Funk  
126 et al., 2015a) precipitation and Global Land Evaporation Amsterdam Model (GLEAM) (Miralles et al., 2011)  
127 evaporation datasets provide high-quality datasets for near-real time drought monitoring. Here, we use  
128 CHIRPS and GLEAM datasets to develop a pan-African high spatial resolution (5-km) SPEI dataset, which  
129 may be useful to inform drought relief management strategies for the continent. The dataset covers the  
130 period from 1981 to 2016 and it is comprehensively inter-compared with soil moisture, vegetation index and  
131 coarse resolution SPEI datasets.

## 132 **2 Data and Methodology**

### 133 **2.1 Data**

#### 134 **2.1.1 CHIRPS**

CHIRPS is a recently-developed high-resolution, daily, pentadal, dekadal, and monthly precipitation dataset (Funk et al., 2015a). It was produced by blending a set of satellite-only precipitation values (CHIRP) with additional monthly and pentadal station observations. The CHIRP is based on infrared cold cloud duration (CCD) estimates calibrated with the Tropical Rainfall Measuring Mission Multi-satellite Precipitation Analysis version 7 (TMPA 3B42 v7) and the Climate Hazards group Precipitation climatology (CHP<sub>clim</sub>). The CHP<sub>clim</sub> (Funk et al., 2015a; Funk et al., 2015e) is based on station data from the Food and Agriculture Organization (FAO) and the Global Historical Climate Network (GHCN). Compared with other global precipitation datasets such as Multi-Source Weighted-Ensemble Precipitation (MSWEP) (Beck et al., 2017) and Global Precipitation Climatology Project (GPCP) (Adler et al., 2003), CHIRPS has several advantages: a long period of record, high spatial resolution (5-km), low spatial biases and low temporal latency. It has been widely validated and applied in various applications (e.g., Shukla et al., 2014; Maidment et al., 2015; Duan et al., 2016; Zambrano-Bigiarini et al., 2017; Rivera et al., 2018). In particular, it was recently validated over East Africa and Mozambique and demonstrated good performance compared to other precipitation datasets (Toté et al., 2015; Dinku et al., 2018). Furthermore, CHIRPS was specifically designed for drought monitoring over regions with deep convective precipitation, scarce observation networks and complex topography (Funk et al., 2014). Several studies (e.g., Toté et al., 2015; Guo et al., 2017) have used CHIRPS for drought monitoring. Its high spatial resolution makes it particularly suitable for local-scale studies, such as sub-basin drought monitoring, especially in areas with complex topography. The detailed description of the dataset was provided by Funk et al. (2015a). In this study, daily CHIRPS precipitation from 1981 to 2016 was used.

### 2.2.2 GLEAM

GLEAM is designed to estimate land surface evaporation and root-zone soil moisture from remote sensing observations and reanalysis data (Miralles et al., 2011; Martens et al., 2017). Specifically, the Priestley-Taylor equation is used to calculate potential evaporation within GLEAM based on near surface temperature and net radiation, while the root zone soil moisture is obtained from a multilayer water balance driven by

precipitation observations and updated with microwave soil moisture estimates (Martens et al., 2017). The actual evaporation is estimated by constraining potential evaporation with a multiplicative evaporative stress factor based on root-zone soil moisture and Vegetation Optical Depth (VOD) estimates. The GLEAM version 3a (v3a) provides global daily potential and actual evaporation, evaporative stress conditions and root zone soil moisture from 1980 to 2018 at spatial resolution of 0.25° (Martens et al., 2017) (see [www.gleam.eu](http://www.gleam.eu)). GLEAM datasets have already been comprehensively evaluated against FLUXNET observations and used for multiple hydro-meteorological applications (Greve et al., 2014; Miralles et al., 2014; Trambauer et al., 2014; Forzieri et al., 2017; Lian et al., 2018; Richard et al., 2018; Vicente-Serrano et al., 2018; Zhan et al., 2019). In particular, two recent studies detected global drought conditions based on GLEAM potential and actual evaporation data (Vicente-Serrano et al., 2018; Peng et al., 2019c). For this study, the GLEAM potential evaporation and root zone soil moisture were used.

#### 2.2.3 CRU-TS

The global gridded CRU-TS datasets provide most widely-used climate variables including precipitation, potential evaporation, diurnal temperature range, maximum and minimum temperature, mean temperature, frost day frequency, cloud cover and vapour pressure (Harris et al., 2014). The CRU TS datasets were produced using angular-distance weighting (ADW) interpolation based on monthly meteorological observations collected at ground-based stations across the world. The recently-released CRU TS version 4.0.1 covers the period 1901–2016 and provides monthly data at 50-km spatial resolution. The CRU TS datasets have been widely used for various applications since their release (e.g., van der Schrier et al., 2013; Chadwick et al., 2015; Delworth et al., 2015; Jägermeyr et al., 2016). The SPEIbase dataset was generated from CRU TS datasets (Beguería et al., 2010). In this study, the CRU TS precipitation and potential evaporation from 1981 to 2016 were used.

#### 2.2.4 GIMMS NDVI

183 The Normalized Difference Vegetation Index (NDVI) can serve as a proxy of vegetation status and has been  
184 widely applied to investigate the effects of drought on vegetation (e.g., Rojas et al., 2011; Vicente-Serrano et  
185 al., 2013; Törnros and Menzel, 2014; Vicente-Serrano et al., 2018). The Global Inventory Monitoring and  
186 Modeling System (GIMMS) NDVI was generated based on Advanced Very High Resolution Radiometer  
187 (AVHRR) observations, and has accounted for various deleterious effects such as orbital drift, calibration  
188 loss and volcanic eruptions (Beck et al., 2011; Pinzon and Tucker, 2014). For the current study, the latest  
189 version of GIMMS NDVI (3g.v1) was used, which covers the time period from 1981 to 2015 at biweekly  
190 temporal resolution and 8-km spatial resolution (Pinzon and Tucker, 2014).

## 191 2.3 Methods

### 192 2.3.1 SPEI calculation

193 The SPEI proposed by Vicente-Serrano et al. (2010) has been used for a wide variety of agricultural,  
194 ecological and hydro-meteorological applications (e.g., Schwalm et al., 2017; Naumann et al., 2018; Jiang et  
195 al., 2019). It accounts for the impacts of evaporation demand on droughts and inherits the simplicity and  
196 multi-temporal characteristics of SPI. The procedure for SPEI calculation includes the estimation of a  
197 climatic water balance (namely the difference between precipitation and potential evaporation), the  
198 aggregation of the climatic water balance over various time-scales (e.g., 1, 3, 6, 12, 24, or more months), and  
199 a fitting to a certain parameter distribution. As suggested by Beguería et al. (2014) and Vicente-Serrano and  
200 Beguería (2016), the log-logistic probability distribution is best for SPEI calculation, from which the  
201 probability distribution of the difference between precipitation and potential evaporation can be calculated as  
202 suggested by Vicente-Serrano et al. (2010) and Beguería et al. (2014). The negative and positive SPEI values  
203 respectively indicate dry and wet conditions. Table 1 summarizes the category of dry and wet conditions  
204 based on SPEI values. In this study, the CHIRPS and GLEAM datasets were used for SPEI calculation at  
205 high spatial resolution (5-km). For comparison, the SPEI at 50-km was also calculated based on CRU TS  
206 datasets for the same 1981–2016 period. It should be noted that the SPEI over sparsely vegetated and barren  
207 areas were masked out based on Moderate Resolution Imaging Spectroradiometer (MODIS) land cover

product (MCD12Q1) (Friedl et al., 2010), because SPEI is not reliable over these areas (Beguería et al., 2010; Beguería et al., 2014; Zhao et al., 2017).

Table 1. Categories of dry and wet conditions indicated by SPEI values.

SPEI	Category
2 and above	Extremely wet
1.5 to 1.99	Very wet
1.0 to 1.49	Moderately wet
-0.99 to 0.99	Near Normal
-1.0 to -1.49	Moderately dry
-1.5 to -1.99	Severely dry
-2 and less	Extremely dry

### 2.3.2 Evaluation criteria

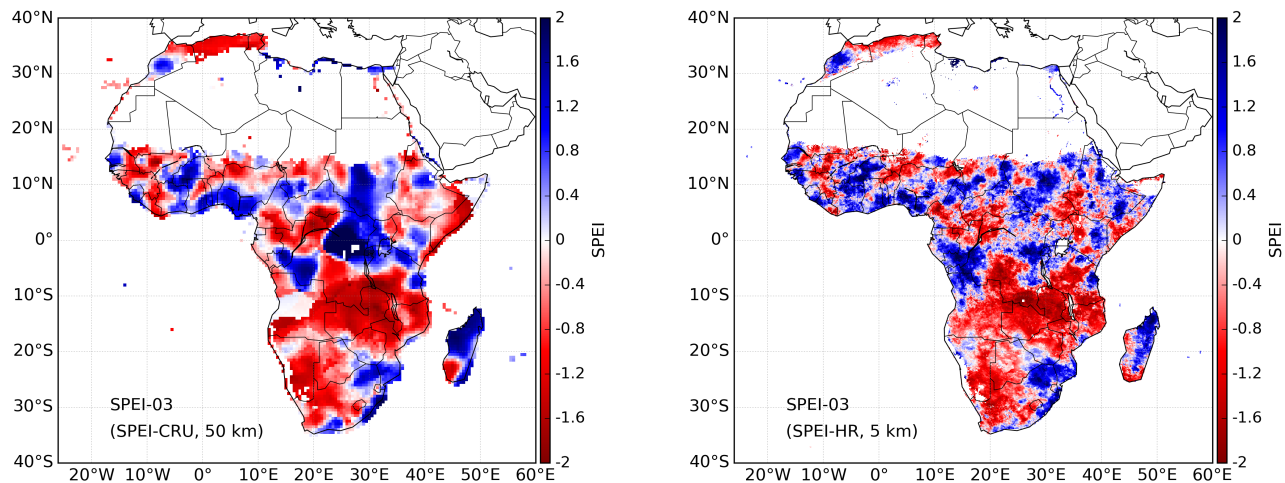
The SPEIbase dataset (Beguería et al., 2010) was calculated with CRU TS dataset, which has been evaluated and applied by many studies (e.g., Chen et al., 2013; Vicente-Serrano et al., 2013; Isbell et al., 2015; Sun et al., 2016a; Greenwood et al., 2017; Um et al., 2017). The newly-generated SPEI at high spatial resolution based on CHIRPS and GLEAM (SPEI-HR) is compared temporally and spatially with the SPEI calculated from CRU TS datasets. In addition, the NDVI can also serve as an indicator for drought and vegetation health, and to assess the performance of drought indices (Vicente-Serrano et al., 2013; Aadhar and Mishra, 2017). Furthermore, root zone soil moisture is an ideal hydrological variable for agricultural (soil moisture) drought monitoring. The recently-released root zone soil moisture (RSM) from GLEAM v3 provides a great opportunity to evaluate whether soil moisture drought is well represented by SPEI. To facilitate direct comparison between SPEI and NDVI as well as RSM, both NDVI and RSM are standardized by subtracting their corresponding (1981–2016) mean and expressed the resulting anomalies as numbers of standard

224 deviations. This standardization has been applied by many studies to evaluate drought indices (Anderson et  
225 al., 2011; Mu et al., 2013; Zhao et al., 2017). The correlation between SPEI and the standardized NDVI and  
226 RSM is quantified using Pearson's correlation coefficient (R). In addition, the high resolution SPEI from  
227 GLEAM and CHIRPS is also resampled to the same grid size of SPEI from CRU TS in order to quantify  
228 their correlation and disentangle whether the added value of the former arises from its increased accuracy or  
229 higher resolution. In the following part, the high (5-km) resolution SPEI is referred to SPEI-HR, while the  
230 coarse 50-km resolution SPEI is referred to SPEI-CRU.

### 231 3 Results and discussion

#### 232 3.1 Inter-comparison between high- and coarse-resolution SPEI

233 Figure 1 shows the spatial distribution of SPEI-HR and SPEI-CRU at different resolutions for an example  
234 month (June 1995). Figure 1a,b show the 3-month SPEI and 12-month SPEI, respectively. It can be seen that  
235 the high resolution and coarse resolution SPEI display quite similar dry and wet patterns over the whole of  
236 Africa for both temporal scales. However, as expected, the SPEI-HR shows much more spatial detail that  
237 reflects mesoscale geographic and climatic features, which highlights the advantages of this new dataset. The  
238 differences in patterns between 3-month and 12-month SPEI indicate the different water deficits caused by  
239 different aggregation time scales, which can further separate agricultural, hydrological, environmental, and  
240 other droughts. For example, in June 1995 southern Africa showed persistent dry conditions over a  
241 prolonged period, while western Africa only showed a short-term drought.



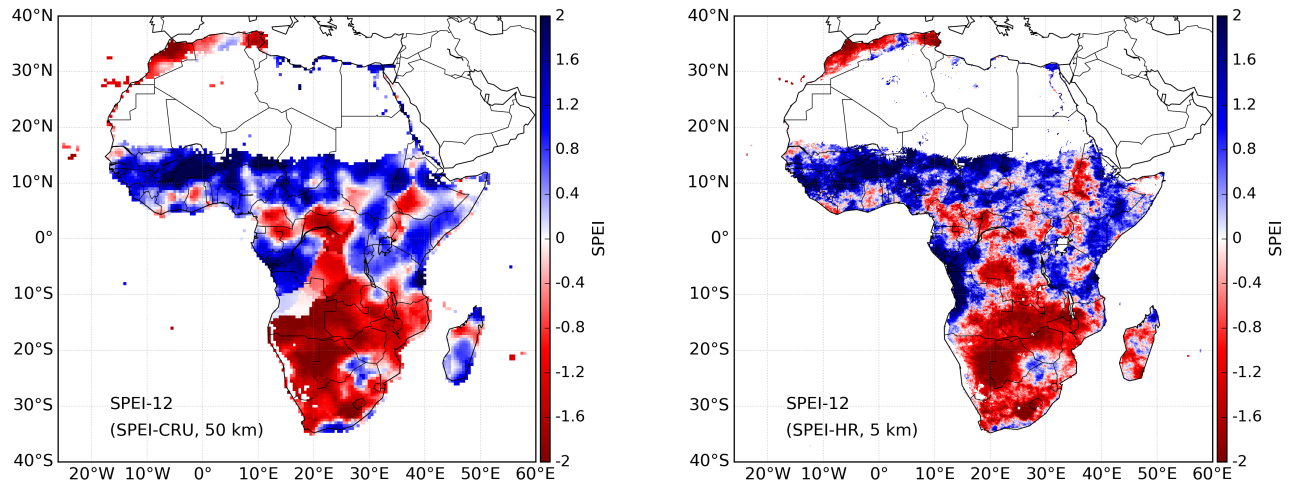
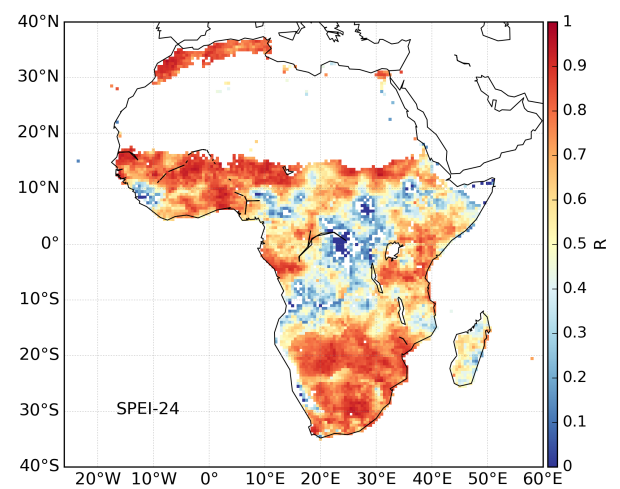
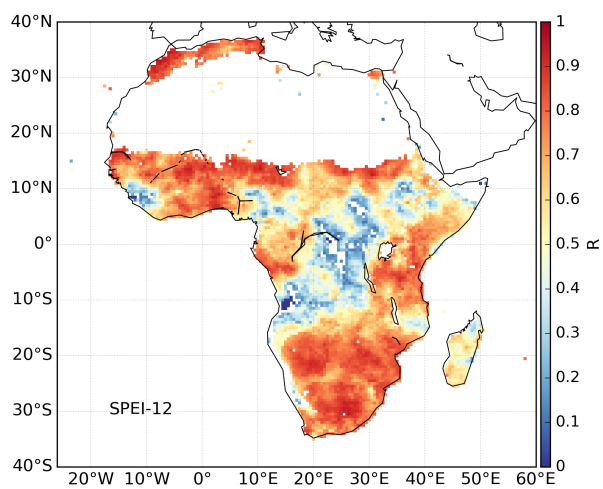
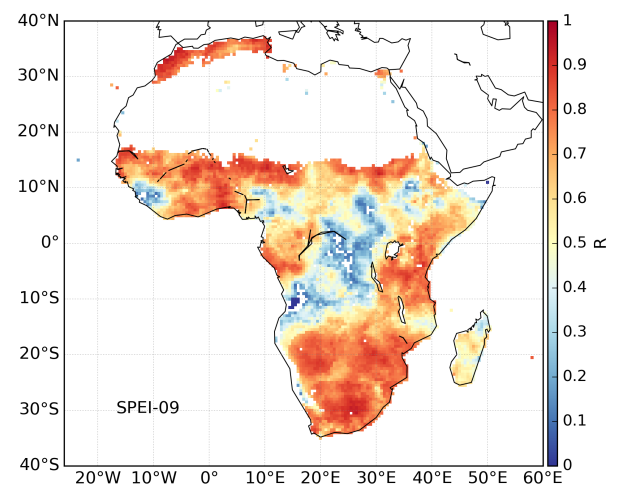
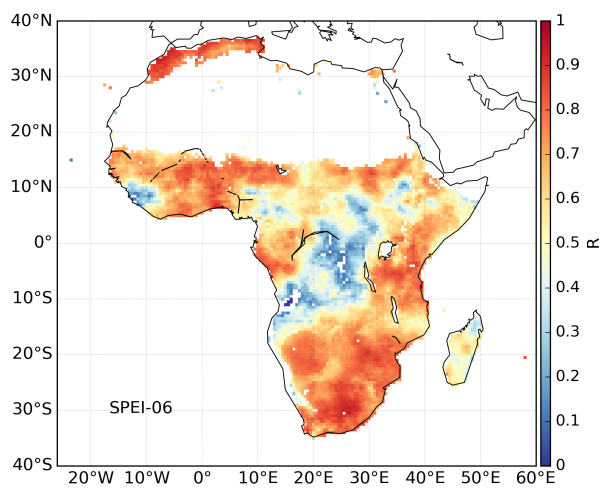
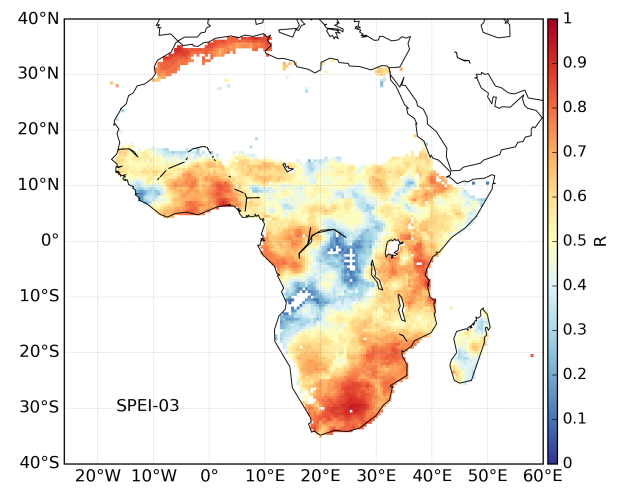
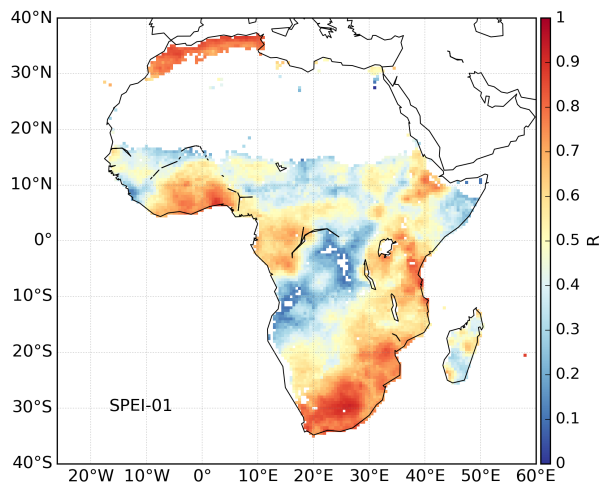


Figure 1: Spatial patterns of 3-month and 12-month SPEI at high spatial resolution (5 km) and coarse spatial resolution (50 km) in June, 1995. The high spatial resolution SPEI (SPEI-HR) is based on CHIRPS precipitation and GLEAM potential evaporation, while the coarse spatial resolution SPEI (SPEI-CRU) is calculated from CRU TS datasets.

In order to quantify how different is SPEI-HR from SPEI-CRU, the correlation between them is calculated for each grid cell over the whole study period. Figure 2 shows the correlations for time-scales 1, 3, 6, 9, 12, 24, 36, and 48 months. In general, the SPEI-HR and SPEI-CRU agree well in terms of temporal variability with high positive correlations over most of Africa for every time scale. However, relatively low correlations appear in central Africa, and they become lower as the SPEI time-scale increases. This region has very few station observations. It should be noted that the correlations shown here are statistically significant with p value less than 0.05. In addition, the average correlation between 6-month SPEI-CRU and SPEI-HR for each month of the year is summarized in Figure 3 using box plot. In general, positive correlations, with a median larger than 0.6 ( $p < 0.05$ ), are found for every month. There are no substantial differences in correlations between different months. Figure A1 in Appendix shows additional box plots for SPEI at other time scales.





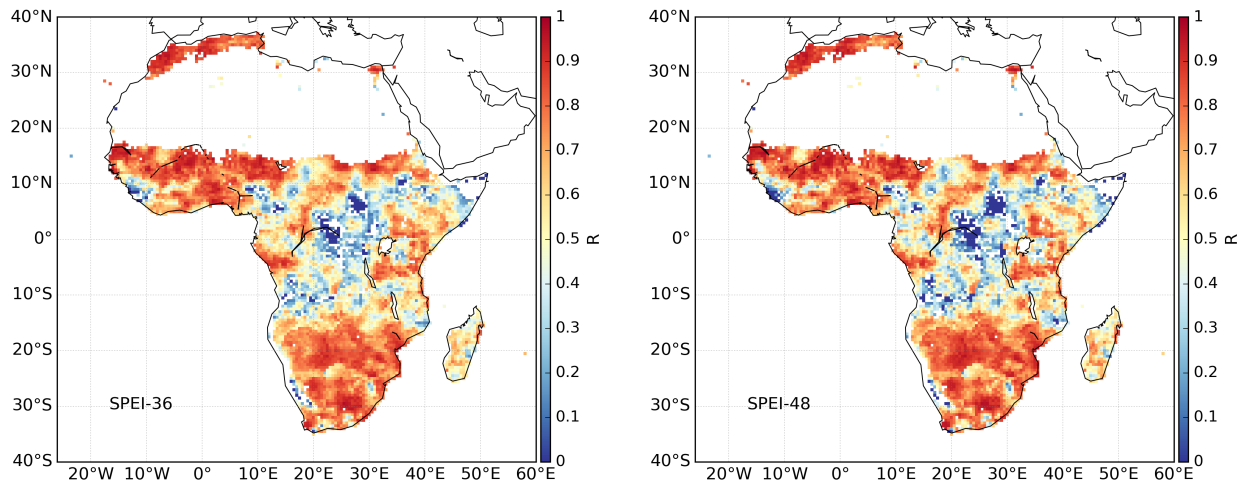


Figure 2: Correlation ( $p<0.05$ ) between SPEI-HR and SPEI-CRU, with the number indicating different months.

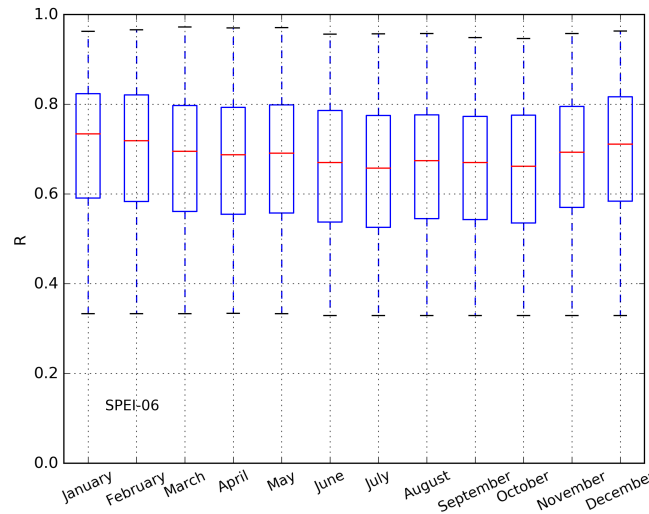


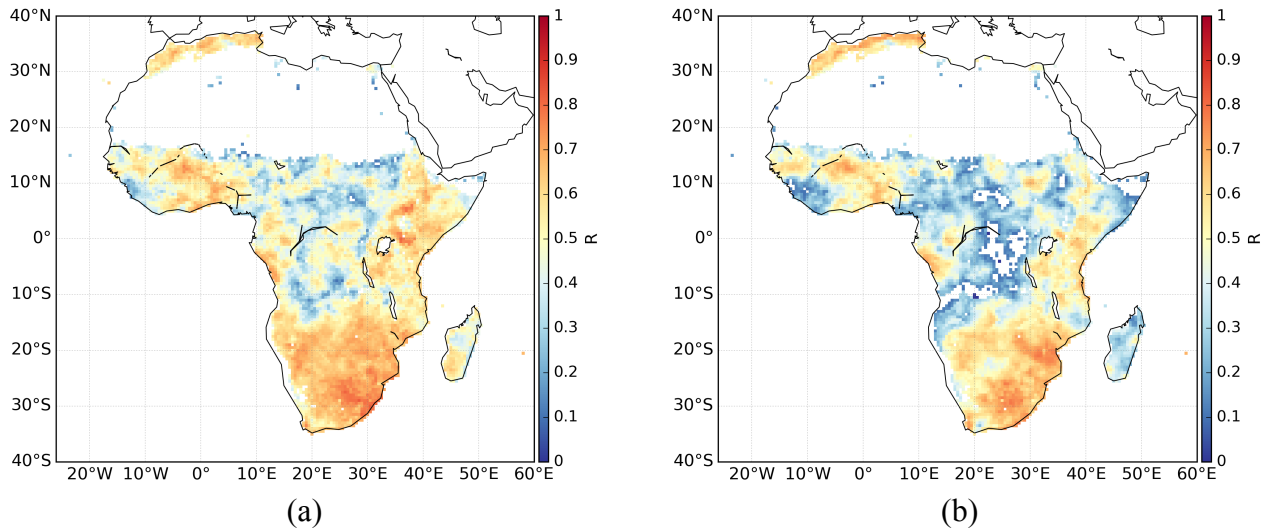
Figure 3: Box plot of the correlation ( $p<0.05$ ) between SPEI-HR and SPEI-CRU for each month of the entire record. The results here are based on 6-month SPEI and the red line in each box represents the median.

### 3.2 Comparison against root zone soil moisture and NDVI

To gain more insights into their significance and applicability, the SPEI datasets are compared with NDVI and RSM. Figure 4 shows the results of the spatial and temporal comparison between 6-month SPEI and RSM as indicated by Törnros and Menzel (2014). Figure 4a,b display the correlation ( $p<0.05$ ) of SPEI-HR and SPEI-CRU against RSM during the whole time period respectively. In general, both SPEI-HR and SPEI-CRU show strong correlations with RSM over the whole African continent. Compared to SPEI-CRU, the SPEI-HR shows higher correlations, particularly over central Africa. Since Section 3.1 shows that relatively

273 large discrepancy between SPEI-CRU and SPEI-HR exists over central Africa, the results presented here  
 274 suggest a potentially better performance of SPEI-HR compared with SPEI-CRU in this region.

275 The time series of SPEI and RSM, averaged over the entire study area, are shown in Figure 4c, together with  
 276 the corresponding correlations. It can be seen that both SPEI-HR and SPEI-CRU agree well with each other  
 277 and with the RSM dynamics. Consistent with the results from the spatial correlation analysis, the SPEI-HR  
 278 and SPEI-CRU show similar results when compared with RSM ( $R = 0.77$  for SPEI-HR,  $R = 0.72$  for SPEI-  
 279 CRU). Furthermore, the scatterplots between 6-month SPEI and RSM for the entire data record are shown in  
 280 Appendix Figure A2, where positive and significant correlations with RSM are found for both SPEI-HR ( $R =$   
 281  $0.51$ ) and SPEI-CRU ( $R = 0.42$ ). To explore the correlation between RSM and different time scales of SPEI,  
 282 Table 2 summarizes the correlation value calculated in the same way as Figure 4c. It can be seen that the  
 283 highest correlations against RSM are found at 3- and 6-month time scales. It should be noted that satellite  
 284 data-driven estimates of root zone soil moisture is more suitable for evaluating SPEI compared to satellite-  
 285 based top-layer soil moisture or reanalysis soil moisture data (Mo et al., 2011; Xu et al., 2018).



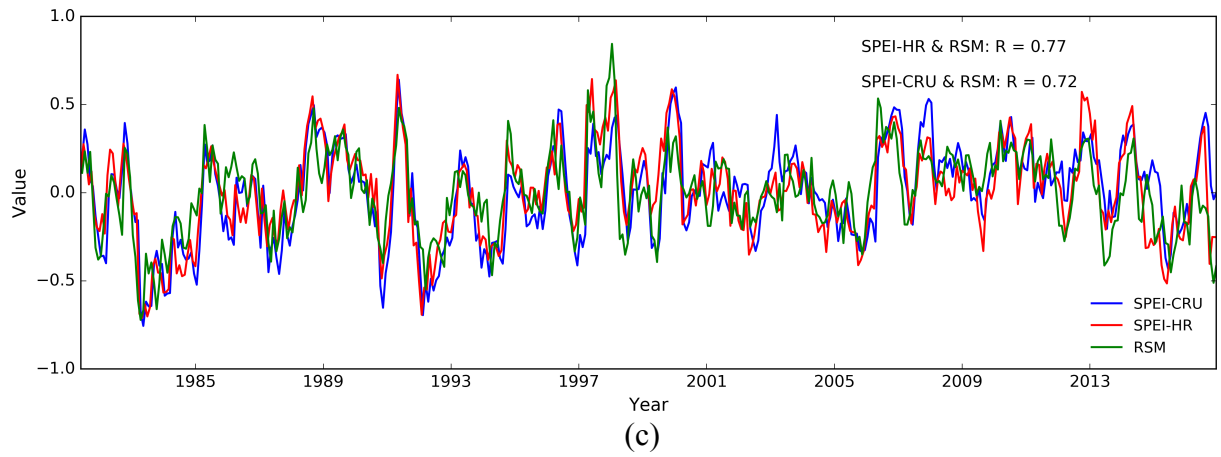


Figure 4: Spatial maps of correlation between SPEI and root zone soil moisture (RSM) for 6-month SPEI: (a) SPEI-HR and (b) SPEI-CRU. The time series of Africa area-mean RSM and SPEI are shown in (c), where R refers to the correlation coefficient. The correlations shown here are all significant at the 95% confidence level.

Table 2: The correlation ( $p < 0.05$ ) between area-mean RSM and SPEI at different time scales.

	SPEI-01	SPEI-03	SPEI-06	SPEI-09	SPEI-12	SPEI-24	SPEI-36	SPEI-48
R (SPEI-CRU)	0.52	0.74	0.72	0.64	0.56	0.41	0.26	0.16
R (SPEI-HR)	0.49	0.76	0.77	0.69	0.62	0.44	0.29	0.18

Similar to the above analysis between SPEI and RSM, the comparison of results between SPEI and NDVI are shown in Figure 5. First, Figures 5a,b present the spatial distribution of the correlations ( $p < 0.05$ ) between SPEI-HR and NDVI and between SPEI-CRU and NDVI, respectively. While correlations are overall lower than for RSM, it can be seen that both SPEI datasets are positively correlated with NDVI over most of the continent. It is also clear that SPEI-HR shows higher correlations. The time series comparison between the area-mean SPEI and NDVI is shown in Figure 5c. Both SPEI-HR and SPEI-CRU show agreement with NDVI, with  $R=0.54$  and  $R=0.47$ , respectively. In addition, the comparison between 6-month SPEI and NDVI for the entire data record was also calculated, with  $R=0.24$  for SPEI-HR and  $R=0.21$  for SPEI-CRU significant at 95% confidence level (Figure A3). While these correlations are admittedly low, overall results suggest that the SPEI has a positive relation with NDVI, which is also reported by previous studies (e.g., Törnros and Menzel, 2014; Vicente-Serrano et al., 2018). The lower correlations against NDVI than against RSM are likely due to complex physiological processes associated to vegetation, and the fact that ecosystem state is driven by multiple variables other than water availability (Nemani et al., 2003). Furthermore, there

are also clearly documented lags between precipitation and NDVI, with NDVI time series typically peaking one or even two months after the period of maximum rainfall (Funk and Brown, 2006). Finally, Table 3 summarizes the correlation between SPEI and NDVI at different time scales. Compared with the results presented in Table 2 for RSM, the correlation with NDVI shown in Table 3 is also generally lower, and the highest correlations appear between 9- and 24-month SPEI ( $R > 0.5$ ).

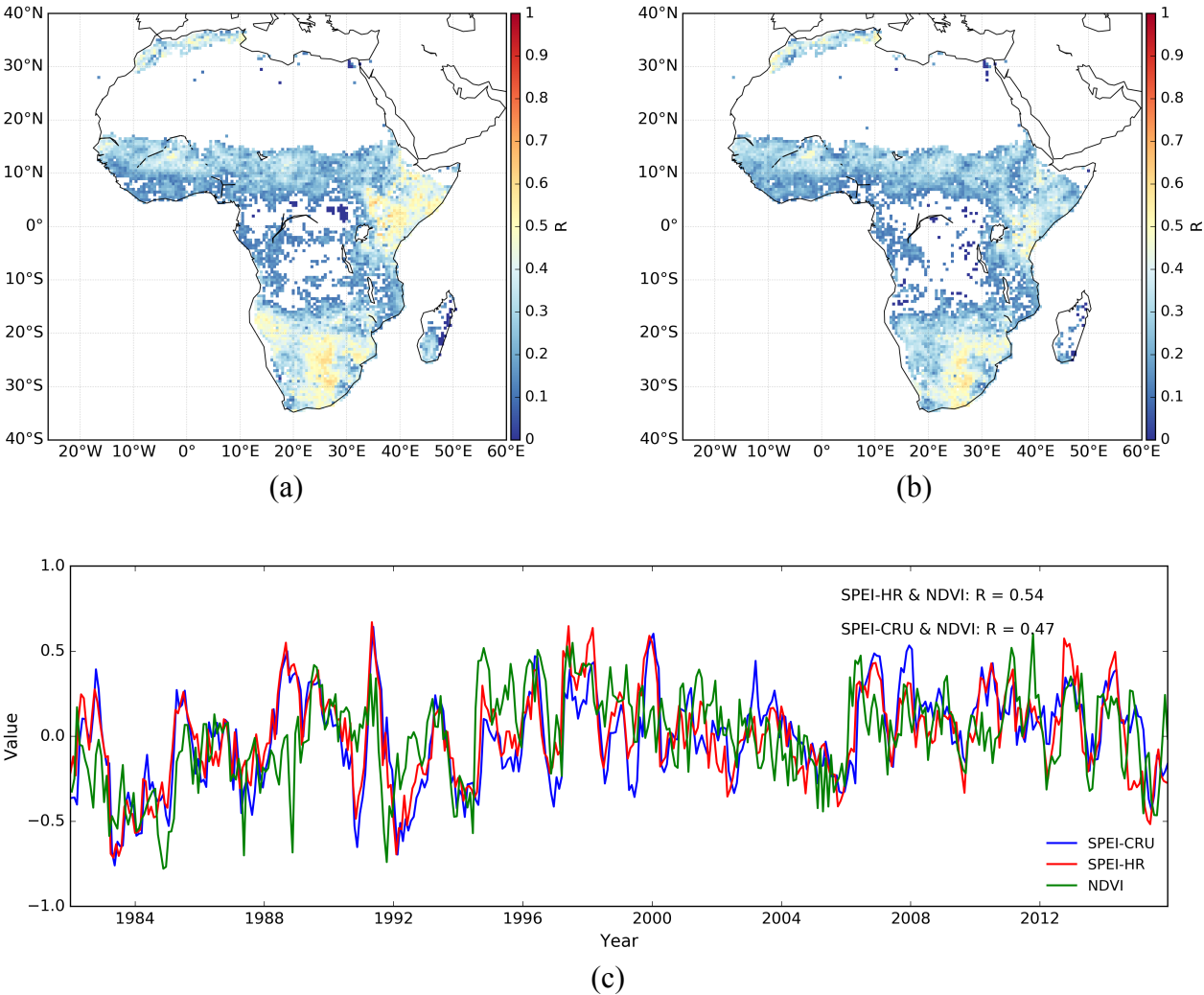


Figure 5: Spatial maps of the correlation between SPEI and NDVI for 6-month SPEI: (a) SPEI-HR and (b) SPEI-CRU. The time series of area-mean NDVI and SPEI are shown in (c), where R refers to the correlation coefficient. The correlations shown here are all significant at the 95% confidence level.

Table 3: The correlation ( $p < 0.05$ ) between area-mean NDVI and SPEI at different time scales.

	SPEI-01	SPEI-03	SPEI-06	SPEI-09	SPEI-12	SPEI-24	SPEI-36	SPEI-48
R (SPEI-CRU)	0.23	0.42	0.47	0.48	0.47	0.50	0.34	0.20
R (SPEI-HR)	0.31	0.51	0.54	0.56	0.57	0.57	0.44	0.29

Altogether, the comparisons between SPEI and RSM and between SPEI and NDVI indirectly indicate the validity of the generated SPEI datasets. Therefore, the generated high-resolution SPEI-HR from satellite products has potential to improve upon the state of the art in drought assessment over Africa.

### 3.3 Patterns of SPEI, RSM and NDVI during specific drought events

Most of Africa has suffered severe droughts in past decades (Naumann et al., 2014; Blamey et al., 2018). Among them, the 2011 East Africa drought (Anderson et al., 2012; AghaKouchak, 2015) and 2002 southern Africa drought (Masih et al., 2014) were extremely severe and had devastating effects on the natural and socioeconomic environment. Taking these two events as case studies, the spatial patterns of the newly-developed high-resolution 6-month SPEI-HR are analyzed, together with the variability in NDVI and RSM. Figure 6a,b show the evolution of 6-month SPEI, NDVI and RSM during the 2011 East Africa and the 2002 southern Africa drought, respectively. The 6-month periods end in the named month, with the 6-month June 2011 SPEI values based on data for January to June. In general, these three variables reflect the progressive dry-out during the events. For example, strong, severe drought is revealed by the SPEI with values less than -1.5, coinciding with a decline in NDVI and RSM, from June to September 2011 over East Africa; the drought was offset in October. Similarly, dry and wet conditions variations during the 2002 southern Africa drought were also captured by the three variables. Despite differences over space and time, results here demonstrate that the generated SPEI-HR captures the main drought conditions that are reflected by negative anomalies in NDVI and RSM, and can thus be used to study local drought related processes and societal impacts in Africa.

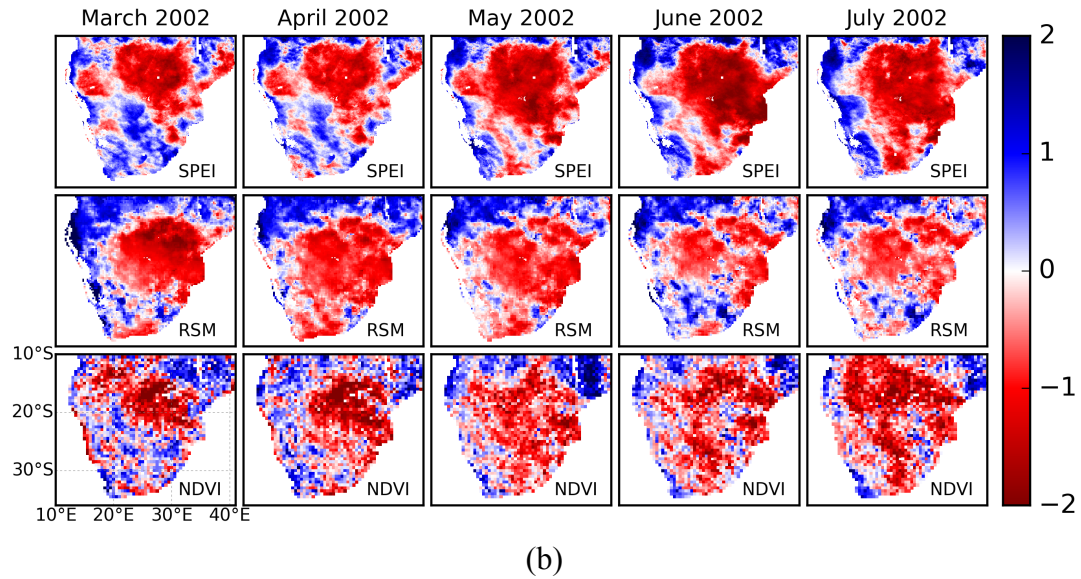
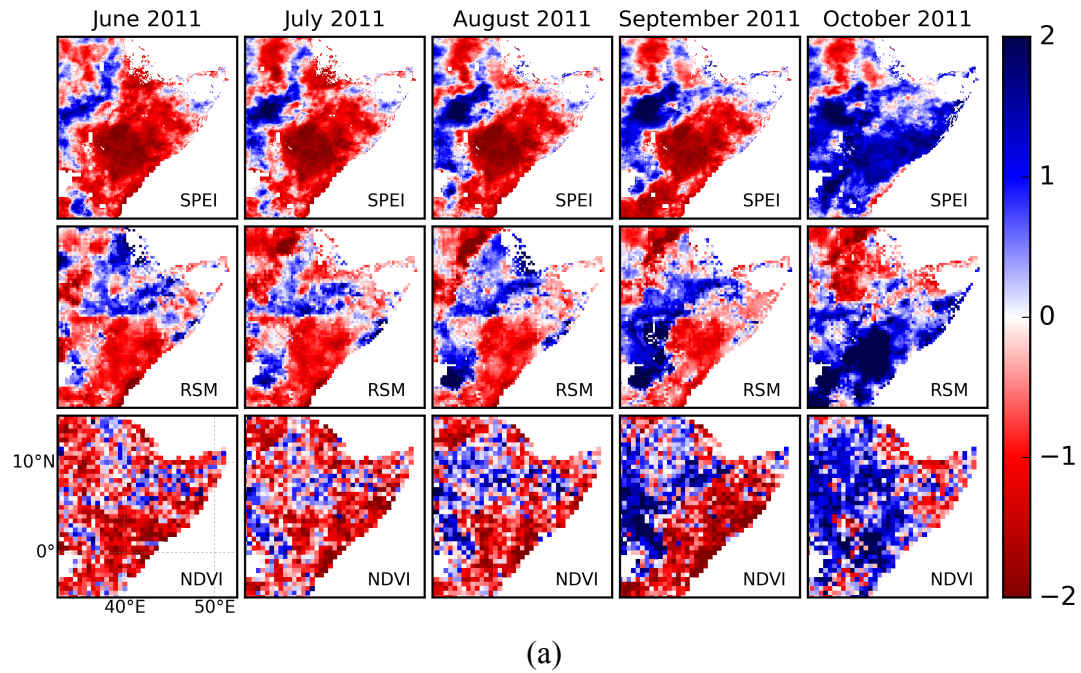


Figure 6: Evolution of the spatial patterns of 6-month SPEI-HR, NDVI and root zone soil moisture (RSM) during the 2011 East Africa drought (a) and 2002 southern Africa drought (b), respectively.

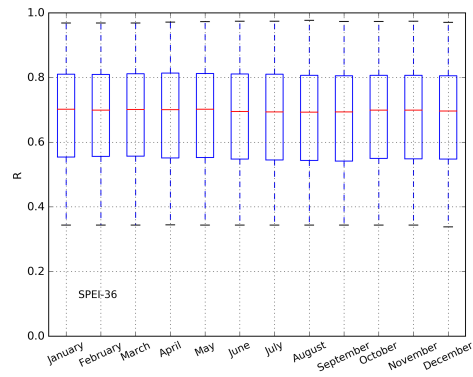
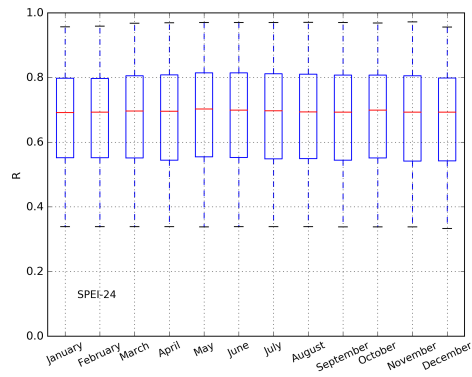
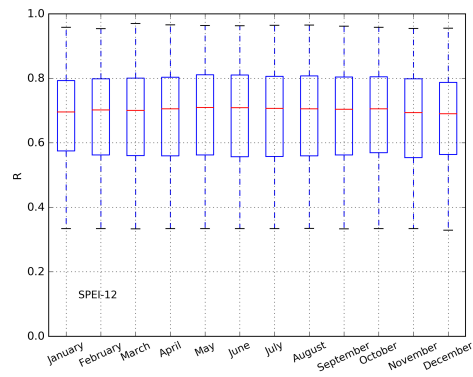
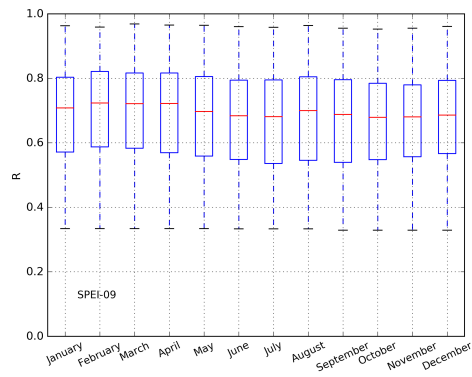
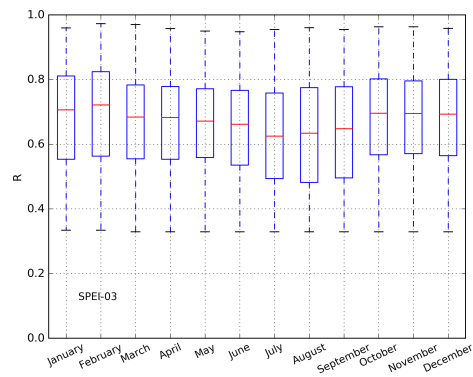
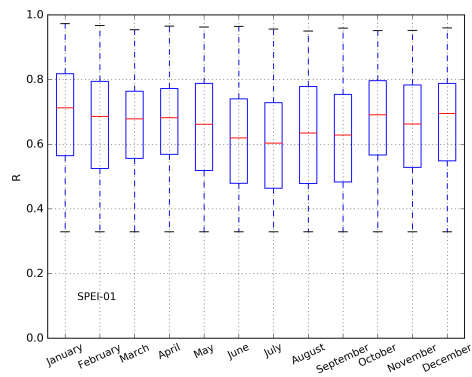
#### 4. Data availability

The high resolution SPEI dataset is publically available from the Centre for Environmental Data Analysis (CEDA) with link: <http://dx.doi.org/10.5285/bbdfd09a04304158b366777eba0d2aeb> (Peng et al., 2019a). It covers the whole Africa at monthly temporal resolution and 5 km spatial resolution from 1981 to 2016, and is provided with Geographic Lat/Lon projection and NetCDF format.

355  
356  
357  
358  
359  
360  
361  
362  
363  
364  
365  
366  
367  
  
368  
  
369  
  
370  
  
371  
  
372  
  
373  
  
374  
  
375  
  
376

## 5. Conclusion

The study presents a newly-generated high-resolution SPEI dataset (SPEI-HR) over Africa. The dataset is produced from satellite-based CHIRPS precipitation and GLEAM potential evaporation, and covers the entire African continent over the time period from 1981 to 2016 with spatial resolution of 5-km. The accumulated SPEI ranging from 1 to 48 months is provided to facilitate applications from meteorological to hydrological droughts. The SPEI-HR was compared with widely used coarse-resolution SPEI data (SPEI-CRU) and GIMMS NDVI as well as GLEAM root zone soil moisture to investigate its capability for drought detection. In general, the SPEI-HR has good correlation with SPEI-CRU temporally and spatially. They both agree well with NDVI and root zone soil moisture, although SPEI-HR displays higher correlations overall. These results indicate the validity and advantage of the newly developed high resolution SPEI-HR dataset, and its unprecedentedly high spatial resolution offers important advantages for drought monitoring and assessment at district and river basin level in Africa.





378

379

380

381

382

383

384

385

386

387

388

389

390

391

392

393

394

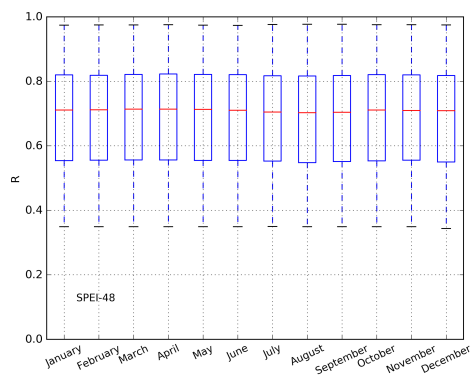


Figure A1: Box plots of the correlation ( $p < 0.05$ ) between SPEI-HR and SPEI-CRU for each month and entire monthly record.

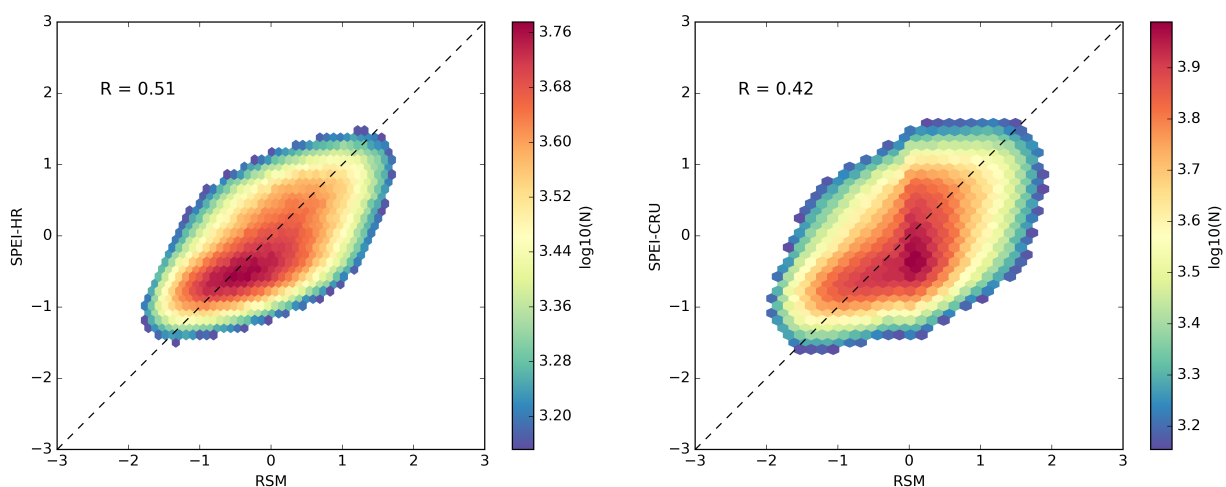
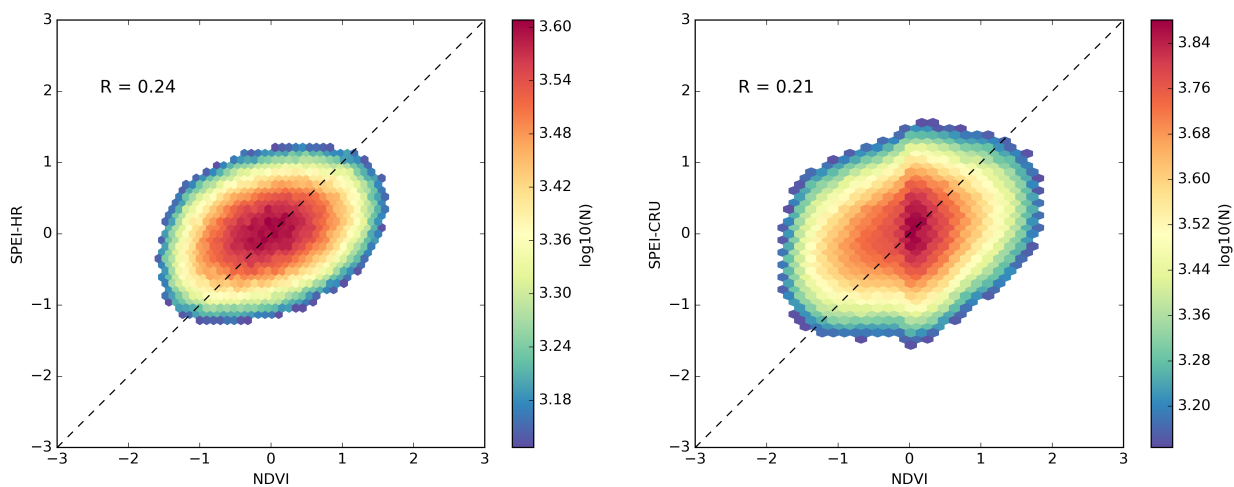


Figure A2: Scatterplots between 6-month SPEI and RSM for the entire data record.  $R$  is correlation coefficient with  $p < 0.05$ , and the colors denote the occurrence frequency of values.



399 Figure A3: Scatterplots between 6-month SPEI and NDVI for the entire data record. R is correlation coefficient with  $p < 0.05$ , and  
400 the colors denote the occurrence frequency of values.  
401

402 **Author contributions**

403 JP developed the processing algorithm, generated the dataset and drafted of the manuscript. DGM and CF  
404 produced the GLEAM and CHIRPS data as input. SD, FH, ED and TL supported the generation of the  
405 dataset and the analysis of the results. All authors contributed to the discussion, review and revision of this  
406 manuscript.

407 **Competing interests**

408 The authors declare that they have no conflict of interest.

409 **Acknowledgments**

410 This work is supported by the UK Space Agency's International Partnership Programme (417000001429).  
411 D.G.M. acknowledges funding from the European Research Council (ERC) under grant agreement 715254  
412 (DRY-2-DRY). SD is also funded by the Natural Environment Research Council (NE/M020339/1). CF is  
413 supported by the U.S. Geological Survey's Drivers of Drought program and NASA Harvest Program grant  
414 Z60592017.

415

418 **References**

- 419 Aadhar, S. and Mishra, V.: High-resolution near real-time drought monitoring in South Asia, *Scientific data*, 4, 170145, 2017.
- 420 Adler, R. F., Huffman, G. J., Chang, A., Ferraro, R., Xie, P.-P., Janowiak, J., Rudolf, B., Schneider, U., Curtis, S., Bolvin, D.,  
 421 Gruber, A., Susskind, J., Arkin, P., and Nelkin, E.: The Version-2 Global Precipitation Climatology Project (GPCP) Monthly  
 422 Precipitation Analysis (1979–Present), *Journal of Hydrometeorology*, 4, 1147–1167, 2003.
- 423 AghaKouchak, A.: A multivariate approach for persistence-based drought prediction: Application to the 2010–2011 East Africa  
 424 drought, *Journal of Hydrology*, 526, 127–135, 2015.
- 425 AghaKouchak, A., Farahmand, A., Melton, F. S., Teixeira, J., Anderson, M. C., Wardlow, B. D., and Hain, C. R.: Remote sensing  
 426 of drought: Progress, challenges and opportunities, *Reviews of Geophysics*, 53, 452–480, 2015.
- 427 Anderson, M. C., Hain, C., Wardlow, B., Pimstein, A., Mecikalski, J. R., and Kustas, W. P.: Evaluation of drought indices based  
 428 on thermal remote sensing of evapotranspiration over the continental United States, *Journal of Climate*, 24, 2025–2044, 2011.
- 429 Anderson, W. B., Zaitchik, B. F., Hain, C. R., Anderson, M. C., Yilmaz, M. T., Mecikalski, J., and Schultz, L.: Towards an  
 430 integrated soil moisture drought monitor for East Africa, *Hydrol. Earth Syst. Sci.*, 16, 2893–2913, 2012.
- 431 Anghileri, D., Li, C., Agaba, G., Kandel, M., Dash, J., Reeves, J., Lewis, L., Hill, C., and Sheffield, J.: Co-production and  
 432 interdisciplinary research in the BRECCIA project: bringing together different expertise and actors for addressing water and food  
 433 security challenges in sub-Saharan Africa, *Geophysical Research Abstracts*2019, EGU2019-14992.
- 434 Arpe, K., Leroy, S., Lahijani, H., and Khan, V.: Impact of the European Russia drought in 2010 on the Caspian Sea level,  
 435 *Hydrology and earth system science*, 16, 19–27, 2012.
- 436 Awange, J. L., Khandu, Schumacher, M., Forootan, E., and Heck, B.: Exploring hydro-meteorological drought patterns over the  
 437 Greater Horn of Africa (1979–2014) using remote sensing and reanalysis products, *Advances in Water Resources*, 94, 45–59,  
 438 2016.
- 439 Bachmair, S., Stahl, K., Collins, K., Hannaford, J., Acreman, M., Svoboda, M., Knutson, C., Smith, K. H., Wall, N., and Fuchs,  
 440 B.: Drought indicators revisited: the need for a wider consideration of environment and society, *Wiley Interdisciplinary Reviews:*  
 441 *Water*, 3, 516–536, 2016.
- 442 Bachmair, S., Tanguy, M., Hannaford, J., and Stahl, K.: How well do meteorological indicators represent agricultural and forest  
 443 drought across Europe?, *Environmental Research Letters*, 13, 034042, 2018.
- 444 Baudoin, M.-A., Vogel, C., Nortje, K., and Naik, M.: Living with drought in South Africa: lessons learnt from the recent El Niño  
 445 drought period, *International Journal of Disaster Risk Reduction*, 23, 128–137, 2017.
- 446 Beck, H. E., McVicar, T. R., van Dijk, A. I., Schellekens, J., de Jeu, R. A., and Bruijnzeel, L. A.: Global evaluation of four  
 447 AVHRR–NDVI data sets: Intercomparison and assessment against Landsat imagery, *Remote Sensing of Environment*, 115, 2547–  
 448 2563, 2011.
- 449 Beck, H. E., Van Dijk, A. I., Levizzani, V., Schellekens, J., Gonzalez Miralles, D., Martens, B., and De Roo, A.: MSWEP: 3-  
 450 hourly 0.25 global gridded precipitation (1979–2015) by merging gauge, satellite, and reanalysis data, *Hydrology and Earth*  
 451 *System Sciences*, 21, 589–615, 2017.
- 452 Becker, A., Finger, P., Meyer-Christoffer, A., Rudolf, B., Schamm, K., Schneider, U., and Ziese, M.: A description of the global  
 453 land-surface precipitation data products of the Global Precipitation Climatology Centre with sample applications including  
 454 centennial (trend) analysis from 1901–present, *Earth System Science Data*, 5, 71–99, 2013.
- 455 Beguería, S., Vicente-Serrano, S. M., and Angulo-Martínez, M.: A multiscalar global drought dataset: the SPEIbase: a new  
 456 gridded product for the analysis of drought variability and impacts, *Bulletin of the American Meteorological Society*, 91, 1351–  
 457 1356, 2010.
- 458 Beguería, S., Vicente-Serrano, S. M., Reig, F., and Latorre, B.: Standardized precipitation evapotranspiration index (SPEI)  
 459 revisited: parameter fitting, evapotranspiration models, tools, datasets and drought monitoring, *International Journal of*  
 460 *Climatology*, 34, 3001–3023, 2014.
- 461 Blamey, R. C., Kolusu, S. R., Mahlalela, P., Todd, M. C., and Reason, C. J. C.: The role of regional circulation features in  
 462 regulating El Niño climate impacts over southern Africa: A comparison of the 2015/2016 drought with previous events,  
 463 *International Journal of Climatology*, 0, 2018.
- 464 Chadwick, R., Good, P., Martin, G., and Rowell, D. P.: Large rainfall changes consistently projected over substantial areas of  
 465 tropical land, *Nature Climate Change*, 6, 177, 2015.
- 466 Chen, T., Werf, G. R., Jeu, R. A. M., Wang, G., and Dolman, A. J.: A global analysis of the impact of drought on net primary  
 467 productivity, *Hydrol. Earth Syst. Sci.*, 17, 3885–3894, 2013.
- 468 Crausbay, S. D., Ramirez, A. R., Carter, S. L., Cross, M. S., Hall, K. R., Bathke, D. J., Betancourt, J. L., Colt, S., Cravens, A. E.,  
 469 and Dalton, M. S.: Defining ecological drought for the twenty-first century, *Bulletin of the American Meteorological Society*, 98,  
 470 2543–2550, 2017.

Dadson, S. J., Lopez, H. P., Peng, J., and Vora, S.: Hydroclimatic Extremes and Climate Change, *Water Science, Policy, and Management: A Global Challenge*, doi: 10.1002/9781119520627.ch2, 2019. 11-28, 2019.

Delworth, T. L., Zeng, F., Rosati, A., Vecchi, G. A., and Wittenberg, A. T.: A Link between the Hiatus in Global Warming and North American Drought, *Journal of Climate*, 28, 3834-3845, 2015.

Deo, R. C., Byun, H.-R., Adamowski, J. F., and Begum, K.: Application of effective drought index for quantification of meteorological drought events: a case study in Australia, *Theoretical and Applied Climatology*, 128, 359-379, 2017.

Ding, Y., Hayes, M. J., and Widhalm, M.: Measuring economic impacts of drought: a review and discussion, *Disaster Prevention and Management: An International Journal*, 20, 434-446, 2011.

Dinku, T., Funk, C., Peterson, P., Maidment, R., Tadesse, T., Gadain, H., and Ceccato, P.: Validation of the CHIRPS satellite rainfall estimates over eastern Africa, *Quarterly Journal of the Royal Meteorological Society*, 0, 2018.

Duan, Z., Liu, J., Tuo, Y., Chiogna, G., and Disse, M.: Evaluation of eight high spatial resolution gridded precipitation products in Adige Basin (Italy) at multiple temporal and spatial scales, *Science of The Total Environment*, 573, 1536-1553, 2016.

Fan, Y. and Van den Dool, H.: A global monthly land surface air temperature analysis for 1948–present, *Journal of Geophysical Research: Atmospheres*, 113, 2008.

Fisher, J. B., Melton, F., Middleton, E., Hain, C., Anderson, M., Allen, R., McCabe, M. F., Hook, S., Baldocchi, D., and Townsend, P. A.: The future of evapotranspiration: Global requirements for ecosystem functioning, carbon and climate feedbacks, agricultural management, and water resources, *Water Resources Research*, 53, 2618-2626, 2017.

Forzieri, G., Alkama, R., Miralles, D. G., and Cescatti, A.: Satellites reveal contrasting responses of regional climate to the widespread greening of Earth, *Science*, 356, 1180-1184, 2017.

Friedl, M. A., Sulla-Menashe, D., Tan, B., Schneider, A., Ramankutty, N., Sibley, A., and Huang, X.: MODIS Collection 5 global land cover: Algorithm refinements and characterization of new datasets, *Remote sensing of Environment*, 114, 168-182, 2010.

Funk, C., Harrison, L., Shukla, S., Pomposi, C., Galu, G., Korecha, D., Husak, G., Magadzire, T., Davenport, F., and Hillbruner, C.: Examining the role of unusually warm Indo-Pacific sea-surface temperatures in recent African droughts, *Quarterly Journal of the Royal Meteorological Society*, 144, 360-383, 2018.

Funk, C., Peterson, P., Landsfeld, M., Pedreros, D., Verdin, J., Shukla, S., Husak, G., Rowland, J., Harrison, L., Hoell, A., and Michaelsen, J.: The climate hazards infrared precipitation with stations—a new environmental record for monitoring extremes, *Scientific Data*, 2, 150066, 2015a.

Funk, C., Verdin, A., Michaelsen, J., Peterson, P., Pedreros, D., and Husak, G.: A global satellite-assisted precipitation climatology, *Earth Syst. Sci. Data*, 7, 275-287, 2015e.

Funk, C. C. and Brown, M. E.: Intra-seasonal NDVI change projections in semi-arid Africa, *Remote Sensing of Environment*, 101, 249-256, 2006.

Funk, C. C., Peterson, P. J., Landsfeld, M. F., Pedreros, D. H., Verdin, J. P., Rowland, J. D., Romero, B. E., Husak, G. J., Michaelsen, J. C., and Verdin, A. P.: A quasi-global precipitation time series for drought monitoring, *US Geological Survey Data Series*, 832, 2014.

García-Herrera, R., Díaz, J., Trigo, R. M., Luterbacher, J., and Fischer, E. M.: A review of the European summer heat wave of 2003, *Critical Reviews in Environmental Science and Technology*, 40, 267-306, 2010.

Gebremeskel, G., Tang, Q., Sun, S., Huang, Z., Zhang, X., and Liu, X.: Droughts in East Africa: Causes, impacts and resilience, *Earth-Science Reviews*, 2019. 2019.

Greenwood, S., Ruiz-Benito, P., Martínez-Vilalta, J., Lloret, F., Kitzberger, T., Allen, C. D., Fensham, R., Laughlin, D. C., Kattge, J., and Bönsch, G.: Tree mortality across biomes is promoted by drought intensity, lower wood density and higher specific leaf area, *Ecology Letters*, 20, 539-553, 2017.

Greve, P., Orlowsky, B., Mueller, B., Sheffield, J., Reichstein, M., and Seneviratne, S. I.: Global assessment of trends in wetting and drying over land, *Nature geoscience*, 7, 716, 2014.

Griffin, D. and Anchukaitis, K. J.: How unusual is the 2012–2014 California drought?, *Geophysical Research Letters*, 41, 9017-9023, 2014.

Guo, H., Bao, A., Liu, T., Ndayisaba, F., He, D., Kurban, A., and De Maeyer, P.: Meteorological drought analysis in the Lower Mekong Basin using satellite-based long-term CHIRPS product, *Sustainability*, 9, 901, 2017.

Harris, I., Jones, P. D., Osborn, T. J., and Lister, D. H.: Updated high-resolution grids of monthly climatic observations – the CRU TS3.10 Dataset, *International Journal of Climatology*, 34, 623-642, 2014.

Heim Jr, R. R.: A review of twentieth-century drought indices used in the United States, *Bulletin of the American Meteorological Society*, 83, 1149-1165, 2002.

Isbell, F., Craven, D., Connolly, J., Loreau, M., Schmid, B., Beierkuhnlein, C., Bezemer, T. M., Bonin, C., Bruehlheide, H., de Luca, E., Ebeling, A., Griffin, J. N., Guo, Q., Hautier, Y., Hector, A., Jentsch, A., Kreyling, J., Lanta, V., Manning, P., Meyer, S. T., Mori, A. S., Naeem, S., Niklaus, P. A., Polley, H. W., Reich, P. B., Roscher, C., Seabloom, E. W., Smith, M. D., Thakur, M. P., Tilman, D., Tracy, B. F., van der Putten, W. H., van Ruijven, J., Weigelt, A., Weisser, W. W., Wilsey, B., and Eisenhauer, N.: Biodiversity increases the resistance of ecosystem productivity to climate extremes, *Nature*, 526, 574, 2015.

Jägermeyr, J., Gerten, D., Schaphoff, S., Heinke, J., Lucht, W., and Rockström, J.: Integrated crop water management might sustainably halve the global food gap, *Environmental Research Letters*, 11, 025002, 2016.

529 Jiang, P., Liu, H., Piao, S., Ciais, P., Wu, X., Yin, Y., and Wang, H.: Enhanced growth after extreme wetness compensates for  
530 post-drought carbon loss in dry forests, *Nature Communications*, 10, 195, 2019.

531 Keyantash, J. and Dracup, J. A.: The quantification of drought: an evaluation of drought indices, *Bulletin of the American*  
532 *Meteorological Society*, 83, 1167-1180, 2002.

533 Kumar, R., Musuza, J. L., Loon, A. F. V., Teuling, A. J., Barthel, R., Ten Broek, J., Mai, J., Samaniego, L., and Attinger, S.:  
534 Multiscale evaluation of the Standardized Precipitation Index as a groundwater drought indicator, *Hydrology and Earth System*  
535 *Sciences*, 20, 1117-1131, 2016.

536 Lian, X., Piao, S., Huntingford, C., Li, Y., Zeng, Z., Wang, X., Ciais, P., McVicar, T. R., Peng, S., Ottlé, C., Yang, H., Yang, Y.,  
537 Zhang, Y., and Wang, T.: Partitioning global land evapotranspiration using CMIP5 models constrained by observations, *Nature*  
538 *Climate Change*, 8, 640-646, 2018.

539 Lloyd-Hughes, B.: The impracticality of a universal drought definition, *Theoretical and Applied Climatology*, 117, 607-611, 2014.

540 Maidment, R. I., Allan, R. P., and Black, E.: Recent observed and simulated changes in precipitation over Africa, *Geophysical*  
541 *Research Letters*, 42, 8155-8164, 2015.

542 Mann, M. E. and Gleick, P. H.: Climate change and California drought in the 21st century, *Proceedings of the National Academy*  
543 *of Sciences*, 112, 3858-3859, 2015.

544 Martens, B., Miralles, D. G., Lievens, H., van der Schalie, R., de Jeu, R. A., Fernández-Prieto, D., Beck, H. E., Dorigo, W. A., and  
545 Verhoest, N. E.: GLEAM v3: satellite-based land evaporation and root-zone soil moisture, *Geoscientific Model Development*, 10,  
546 1903, 2017.

547 Marvel, K., Cook, B. I., Bonfils, C. J., Durack, P. J., Smerdon, J. E., and Williams, A. P.: Twentieth-century hydroclimate changes  
548 consistent with human influence, *Nature*, 569, 59, 2019.

549 Masih, I., Maskey, S., Mussá, F., and Trambauer, P.: A review of droughts on the African continent: a geospatial and long-term  
550 perspective, *Hydrology and Earth System Sciences*, 18, 3635-3649, 2014.

551 McKee, T. B., Doesken, N. J., and Kleist, J.: The relationship of drought frequency and duration to time scales, 1993, 179-183.

552 Miralles, D. G., Holmes, T. R. H., De Jeu, R. A. M., Gash, J. H., Meesters, A. G. C. A., and Dolman, A. J.: Global land-surface  
553 evaporation estimated from satellite-based observations, *Hydrol. Earth Syst. Sci.*, 15, 453-469, 2011.

554 Miralles, D. G., Van Den Berg, M. J., Gash, J. H., Parinussa, R. M., De Jeu, R. A., Beck, H. E., Holmes, T. R., Jiménez, C.,  
555 Verhoest, N. E., and Dorigo, W. A.: El Niño–La Niña cycle and recent trends in continental evaporation, *Nature Climate Change*,  
556 4, 122, 2014.

557 Mishra, A. K. and Singh, V. P.: A review of drought concepts, *Journal of hydrology*, 391, 202-216, 2010.

558 Mo, K. C., Long, L. N., Xia, Y., Yang, S. K., Schemm, J. E., and Ek, M.: Drought Indices Based on the Climate Forecast System  
559 Reanalysis and Ensemble NLDAS, *Journal of Hydrometeorology*, 12, 181-205, 2011.

560 Mu, Q., Zhao, M., Kimball, J. S., McDowell, N. G., and Running, S. W.: A remotely sensed global terrestrial drought severity  
561 index, *Bulletin of the American Meteorological Society*, 94, 83-98, 2013.

562 Mukherjee, S., Mishra, A., and Trenberth, K. E.: Climate change and drought: a perspective on drought indices, *Current Climate*  
563 *Change Reports*, 4, 145-163, 2018.

564 Muller, M.: Cape Town's drought: don't blame climate change. Nature Publishing Group, 2018.

565 Naumann, G., Alfieri, L., Wyser, K., Mentaschi, L., Betts, R. A., Carrao, H., Spinoni, J., Vogt, J., and Feyen, L.: Global Changes  
566 in Drought Conditions Under Different Levels of Warming, *Geophysical Research Letters*, 45, 3285-3296, 2018.

567 Naumann, G., Dutra, E., Barbosa, P., Pappenberger, F., Wetterhall, F., and Vogt, J.: Comparison of drought indicators derived  
568 from multiple data sets over Africa, *Hydrology and Earth System Sciences*, 18, 1625-1640, 2014.

569 Nemani, R. R., Keeling, C. D., Hashimoto, H., Jolly, W. M., Piper, S. C., Tucker, C. J., Myneni, R. B., and Running, S. W.:  
570 Climate-Driven Increases in Global Terrestrial Net Primary Production from 1982 to 1999, *Science*, 300, 1560-1563, 2003.

571 Nicholson, S. E.: A detailed look at the recent drought situation in the Greater Horn of Africa, *Journal of Arid Environments*, 103,  
572 71-79, 2014.

573 Nicholson, S. E.: The ITCZ and the seasonal cycle over equatorial Africa, *Bulletin of the American Meteorological Society*, 99,  
574 337-348, 2018.

575 Panu, U. and Sharma, T.: Challenges in drought research: some perspectives and future directions, *Hydrological Sciences Journal*,  
576 47, S19-S30, 2002.

577 Peña-Gallardo, M., Vicente-Serrano, S., Camarero, J., Gazol, A., Sánchez-Salguero, R., Domínguez-Castro, F., El Kenawy, A.,  
578 Beguería-Portugés, S., Gutiérrez, E., and de Luis, M.: Drought Sensitiveness on Forest Growth in Peninsular Spain and the  
579 Balearic Islands, *Forests*, 9, 524, 2018a.

580 Peña-Gallardo, M., Vicente-Serrano, S. M., Domínguez-Castro, F., Quiring, S., Svoboda, M., Beguería, S., and Hannaford, J.:  
581 Effectiveness of drought indices in identifying impacts on major crops across the USA, *Climate Research*, 75, 221-240, 2018b.

582 Peng, J., Dadson, S., Hirpa, F., Dyer, E., Lees, T., Miralles, D. G., Vicente-Serrano, S. M. V.-S., and Funk, C.: High resolution  
583 Standardized Precipitation Evapotranspiration Index (SPEI) dataset for Africa, Centre for Environmental Data Analysis, doi:  
584 10.5285/bbdf09a04304158b366777eba0d2aeb. , 2019a. 2019a.

585 Peng, J., Dadson, S., Leng, G., Duan, Z., Jagdhuber, T., Guo, W., and Ludwig, R.: The impact of the Madden-Julian Oscillation on  
586 hydrological extremes, *Journal of Hydrology*, 571, 142-149, 2019c.

587 Peng, J., Muller, J.-P., Blessing, S., Giering, R., Danne, O., Gobron, N., Kharbouche, S., Ludwig, R., Müller, B., and Leng, G.:  
 588 Can We Use Satellite-Based FAPAR to Detect Drought?, *Sensors*, 19, 3662, 2019d.  
 589 Pinzon, J. E. and Tucker, C. J.: A non-stationary 1981–2012 AVHRR NDVI3g time series, *Remote Sensing*, 6, 6929–6960, 2014.  
 590 Pozzi, W., Sheffield, J., Stefanski, R., Cripe, D., Pulwarty, R., Vogt, J. V., Heim Jr, R. R., Brewer, M. J., Svoboda, M., and  
 591 Westerhoff, R.: Toward global drought early warning capability: Expanding international cooperation for the development of a  
 592 framework for monitoring and forecasting, *Bulletin of the American Meteorological Society*, 94, 776–785, 2013.  
 593 Richard, W., Sonia, I. S., Martin, H., Jinfeng, C., Philippe, C., Delphine, D., Joshua, E., Christian, F., Simon, N. G., Lukas, G.,  
 594 Alexandra-Jane, H., Thomas, H., Akihiko, I., Nikolay, K., Hyungjun, K., Guoyong, L., Junguo, L., Xingcai, L., Yoshimitsu, M.,  
 595 Catherine, M., Christoph, M., Hannes Müller, S., Kazuya, N., Rene, O., Yadu, P., Thomas, A. M. P., Yusuke, S., Sibyll, S., Erwin,  
 596 S., Justin, S., Tobias, S., Joerg, S., Qiuhong, T., Wim, T., Yoshihide, W., Xuhui, W., Graham, P. W., Hong, Y., and Tian, Z.:  
 597 Evapotranspiration simulations in ISIMIP2a—Evaluation of spatio-temporal characteristics with a comprehensive ensemble of  
 598 independent datasets, *Environmental Research Letters*, 13, 075001, 2018.  
 599 Rivera, J. A., Marianetti, G., and Hinrichs, S.: Validation of CHIRPS precipitation dataset along the Central Andes of Argentina,  
 600 *Atmospheric Research*, 213, 437–449, 2018.  
 601 Rojas, O., Vrieling, A., and Rembold, F.: Assessing drought probability for agricultural areas in Africa with coarse resolution  
 602 remote sensing imagery, *Remote sensing of Environment*, 115, 343–352, 2011.  
 603 Schneider, U., Ziese, M., Meyer-Christoffer, A., Finger, P., Rustemeier, E., and Becker, A.: The new portfolio of global  
 604 precipitation data products of the Global Precipitation Climatology Centre suitable to assess and quantify the global water cycle  
 605 and resources, *Proceedings of the International Association of Hydrological Sciences*, 374, 29–34, 2016.  
 606 Schwalm, C. R., Anderegg, W. R. L., Michalak, A. M., Fisher, J. B., Biondi, F., Koch, G., Litvak, M., Ogle, K., Shaw, J. D., Wolf,  
 607 A., Huntzinger, D. N., Schaefer, K., Cook, R., Wei, Y., Fang, Y., Hayes, D., Huang, M., Jain, A., and Tian, H.: Global patterns of  
 608 drought recovery, *Nature*, 548, 202, 2017.  
 609 Sheffield, J., Wood, E. F., Chaney, N., Guan, K., Sadri, S., Yuan, X., Olang, L., Amani, A., Ali, A., and Demuth, S.: A drought  
 610 monitoring and forecasting system for sub-Sahara African water resources and food security, *Bulletin of the American  
 611 Meteorological Society*, 95, 861–882, 2014.  
 612 Shukla, S., McNally, A., Husak, G., and Funk, C.: A seasonal agricultural drought forecast system for food-insecure regions of  
 613 East Africa, *Hydrology and Earth System Sciences*, 18, 3907–3921, 2014.  
 614 Spinoni, J., Naumann, G., Vogt, J. V., and Barbosa, P.: The biggest drought events in Europe from 1950 to 2012, *Journal of  
 615 Hydrology: Regional Studies*, 3, 509–524, 2015.  
 616 Sun, Q., Miao, C., AghaKouchak, A., and Duan, Q.: Century-scale causal relationships between global dry/wet conditions and the  
 617 state of the Pacific and Atlantic Oceans, *Geophysical Research Letters*, 43, 6528–6537, 2016a.  
 618 Sun, S., Chen, H., Li, J., Wei, J., Wang, G., Sun, G., Hua, W., Zhou, S., and Deng, P.: Dependence of 3-month Standardized  
 619 Precipitation-Evapotranspiration Index dryness/wetness sensitivity on climatological precipitation over southwest China,  
 620 *International Journal of Climatology*, 38, 4568–4578, 2018.  
 621 Sun, S., Chen, H., Wang, G., Li, J., Mu, M., Yan, G., Xu, B., Huang, J., Wang, J., and Zhang, F.: Shift in potential  
 622 evapotranspiration and its implications for dryness/wetness over Southwest China, *Journal of Geophysical Research:  
 623 Atmospheres*, 121, 9342–9355, 2016c.  
 624 Swain, D. L., Tsiang, M., Haugen, M., Singh, D., Charland, A., Rajaratnam, B., and Diffenbaugh, N. S.: The extraordinary  
 625 California drought of 2013/2014: Character, context, and the role of climate change, *Bull. Am. Meteorol. Soc.*, 95, S3–S7, 2014.  
 626 Törnros, T. and Menzel, L.: Addressing drought conditions under current and future climates in the Jordan River region,  
 627 *Hydrology and Earth System Sciences*, 18, 305–318, 2014.  
 628 Toté, C., Patricio, D., Boogaard, H., Van Der Wijngaart, R., Tarnavsky, E., and Funk, C.: Evaluation of satellite rainfall estimates  
 629 for drought and flood monitoring in Mozambique, *Remote Sensing*, 7, 1758–1776, 2015.  
 630 Trambauer, P., Dutra, E., Maskey, S., Werner, M., Pappenberger, F., Van Beek, L., and Uhlenbrook, S.: Comparison of different  
 631 evaporation estimates over the African continent, *Hydrology and Earth System Sciences*, 18, 193–212, 2014.  
 632 Trambauer, P., Maskey, S., Winsemius, H., Werner, M., and Uhlenbrook, S.: A review of continental scale hydrological models  
 633 and their suitability for drought forecasting in (sub-Saharan) Africa, *Physics and Chemistry of the Earth, Parts A/B/C*, 66, 16–26,  
 634 2013.  
 635 Um, M.-J., Kim, Y., Park, D., and Kim, J.: Effects of different reference periods on drought index (SPEI) estimations from 1901 to  
 636 2014, *Hydrology & Earth System Sciences*, 21, 2017.  
 637 van der Schrier, G., Barichivich, J., Briffa, K., and Jones, P.: A scPDSI-based global data set of dry and wet spells for 1901–2009,  
 638 *Journal of Geophysical Research: Atmospheres*, 118, 4025–4048, 2013.  
 639 van Dijk, A. I., Beck, H. E., Crosbie, R. S., de Jeu, R. A., Liu, Y. Y., Podger, G. M., Timbal, B., and Viney, N. R.: The  
 640 Millennium Drought in southeast Australia (2001–2009): Natural and human causes and implications for water resources,  
 641 ecosystems, economy, and society, *Water Resources Research*, 49, 1040–1057, 2013.  
 642 Van Loon, A. F.: *Hydrological drought explained*, Wiley Interdisciplinary Reviews: Water, 2, 359–392, 2015.  
 643 Vicente-Serrano, S.: Foreword: Drought complexity and assessment under climate change conditions, *Cuadernos de Investigación  
 644 Geográfica*, 42, 7–11, 2016.

645 Vicente-Serrano, S. M.: Evaluating the impact of drought using remote sensing in a Mediterranean, semi-arid region, *Natural*  
 646 *Hazards*, 40, 173-208, 2007.  
 647 Vicente-Serrano, S. M. and Beguería, S.: Comment on ‘Candidate distributions for climatological drought indices (SPI and SPEI)’  
 648 by James H. Stagge et al, *International Journal of Climatology*, 36, 2120-2131, 2016.  
 649 Vicente-Serrano, S. M., Beguería, S., Gimeno, L., Eklundh, L., Giuliani, G., Weston, D., El Kenawy, A., López-Moreno, J. I.,  
 650 Nieto, R., and Ayenew, T.: Challenges for drought mitigation in Africa: The potential use of geospatial data and drought  
 651 information systems, *Applied Geography*, 34, 471-486, 2012a.  
 652 Vicente-Serrano, S. M., Beguería, S., and López-Moreno, J. I.: A multiscalar drought index sensitive to global warming: the  
 653 standardized precipitation evapotranspiration index, *Journal of climate*, 23, 1696-1718, 2010.  
 654 Vicente-Serrano, S. M., Beguería, S., Lorenzo-Lacruz, J., Camarero, J. J., López-Moreno, J. I., Azorin-Molina, C., Revuelto, J.,  
 655 Morán-Tejeda, E., and Sanchez-Lorenzo, A.: Performance of Drought Indices for Ecological, Agricultural, and Hydrological  
 656 Applications, *Earth Interactions*, 16, 1-27, 2012b.  
 657 Vicente-Serrano, S. M., García-Herrera, R., Barriopedro, D., Azorin-Molina, C., López-Moreno, J. I., Martín-Hernández, N.,  
 658 Tomás-Burguera, M., Gimeno, L., and Nieto, R.: The Westerly Index as complementary indicator of the North Atlantic oscillation  
 659 in explaining drought variability across Europe, *Climate Dynamics*, 47, 845-863, 2016.  
 660 Vicente-Serrano, S. M., Gouveia, C., Camarero, J. J., Beguería, S., Trigo, R., López-Moreno, J. I., Azorín-Molina, C., Pasho, E.,  
 661 Lorenzo-Lacruz, J., Revuelto, J., Morán-Tejeda, E., and Sanchez-Lorenzo, A.: Response of vegetation to drought time-scales  
 662 across global land biomes, *Proceedings of the National Academy of Sciences*, 110, 52-57, 2013.  
 663 Vicente-Serrano, S. M., Miralles, D. G., Domínguez-Castro, F., Azorin-Molina, C., Kenawy, A. E., McVicar, T. R., Tomás-  
 664 Burguera, M., Beguería, S., Maneta, M., and Peña-Gallardo, M.: Global Assessment of the Standardized Evapotranspiration  
 665 Deficit Index (SEDI) for Drought Analysis and Monitoring, *Journal of Climate*, 31, 5371-5393, 2018.  
 666 Vicente-Serrano, S. M., Tomas-Burguera, M., Beguería, S., Reig, F., Latorre, B., Peña-Gallardo, M., Luna, M. Y., Morata, A., and  
 667 González-Hidalgo, J. C.: A high resolution dataset of drought indices for Spain, *Data*, 2, 22, 2017.  
 668 von Hardenberg, J., Meron, E., Shachak, M., and Zarmi, Y.: Diversity of vegetation patterns and desertification, *Physical Review*  
 669 *Letters*, 87, 198101, 2001.  
 670 Wang, H. and He, S.: The North China/Northeastern Asia Severe Summer Drought in 2014, *Journal of Climate*, 28, 6667-6681,  
 671 2015.  
 672 Wegren, S. K.: Food security and Russia's 2010 drought, *Eurasian Geography and Economics*, 52, 140-156, 2011.  
 673 Wilhite, D. and Pulwarty, R.: Drought as Hazard: Understanding the Natural and Social Context. In: *Drought and Water Crises:*  
 674 *Integrating Science, Management, and Policy*, 2017.  
 675 Wilhite, D. A., Svoboda, M. D., and Hayes, M. J.: Understanding the complex impacts of drought: A key to enhancing drought  
 676 mitigation and preparedness, *Water resources management*, 21, 763-774, 2007.  
 677 Xu, Y., Wang, L., Ross, K. W., Liu, C., and Berry, K.: Standardized Soil Moisture Index for Drought Monitoring Based on Soil  
 678 Moisture Active Passive Observations and 36 Years of North American Land Data Assimilation System Data: A Case Study in the  
 679 Southeast United States, *Remote Sensing*, 10, 301, 2018.  
 680 Yuan, X., Wood, E. F., Chaney, N. W., Sheffield, J., Kam, J., Liang, M., and Guan, K.: Probabilistic Seasonal Forecasting of  
 681 African Drought by Dynamical Models, *Journal of Hydrometeorology*, 14, 1706-1720, 2013.  
 682 Zambrano-Bigiarini, M., Nauditt, A., Birkel, C., Verbist, K., and Ribbe, L.: Temporal and spatial evaluation of satellite-based  
 683 rainfall estimates across the complex topographical and climatic gradients of Chile, *Hydrology and Earth System Sciences*, 21,  
 684 1295-1320, 2017.  
 685 Zhan, S., Song, C., Wang, J., Sheng, Y., and Quan, J.: A global assessment of terrestrial evapotranspiration increase due to surface  
 686 water area change, *Earth's future*, 7, 266-282, 2019.  
 687 Zhao, M., A, G., Velicogna, I., and Kimball, J. S.: A Global Gridded Dataset of GRACE Drought Severity Index for 2002–14:  
 688 Comparison with PDSI and SPEI and a Case Study of the Australia Millennium Drought, *Journal of Hydrometeorology*, 18, 2117-  
 689 2129, 2017.  
 690 Zhou, Q., Leng, G., and Peng, J.: Recent Changes in the Occurrences and Damages of Floods and Droughts in the United States,  
 691 *Water*, 10, 1109, 2018.  
 692 Ziese, M., Schneider, U., Meyer-Christoffer, A., Schamm, K., Vido, J., Finger, P., Bissolli, P., Pietzsch, S., and Becker, A.: The  
 693 GPCC Drought Index—a new, combined and gridded global drought index, *Earth System Science Data*, 6, 285-295, 2014.

694

695